Phenomenology of the Lightest Pseudo-Nambu-Goldstone Boson of a Dynamical Symmetry Breaking Model

J. F Gunion, Keystone LC Workshop, September 26–29, 1998

Collaborators: R. Casalbuoni, A. Deandrea, S. De Curtis, D. Dominici, and R. Gatto.

Reference: UCD-98-13, hep-ph/9809523

TOPICS

- Defining the model: lagrangian; eigenstates; couplings.
- Expectations from Tevatron and LHC.
- The role of the NLC.
- Implications for machines and detectors.

1 The Model

Phrase in terms of effective Lagrangian, but think technicolor ($U_{1,2,3}, D_{1,2,3}, N, E$) ($1, 2, 3 =$ color indices) — *i.e.* 8 fields from a flavor-color perspective.

- In one-family model one begins with an underlying $SU(8)_L \times SU(8)_R$ symmetry. When one introduces dynamical symmetry breaking resulting in non-zero $\langle U\overline{U}\rangle$, $\langle D\overline{D}\rangle$ (internal color sums implicit), $\langle N\overline{N}\rangle$ and $\langle E\overline{E}\rangle$,

  $\Rightarrow$ breaks to $SU(8)_V$, leaving behind $8 \times 8 - 1 = 63$ PNGB's, which are pseudo-scalars (unlike scalar Higgs boson). These are massless until non-technicolor interactions are introduced.

  - 32 are color octets.
  - 24 are color triplets.
  - 3 are absorbed to give $W^\pm, Z$ masses.
  - 2 are color neutral but charged.
  - 2 are color neutral *and* chargeless.

- The masses of the dynamically formed resonances, ρ_T, ω_T *etc.*, will generally be $\gtrsim$ TeV.

- The masses of the colored objects will also be quite large.

- The masses of the 4 colorless PNGB's will be smallest.

  $\Rightarrow$ focus on them.

- Of these, it will turn that one, which we shall denote P^0 will have much smaller mass than the others.

$m_{P^0} \leq 100$ GeV is probable, whereas the others almost certainly have masses ≥ 200 GeV.

- The effective Lagrangian describing the PNGB's has two pieces: gauge and Yukawa.

$$\mathcal{L}_g = \frac{v^2}{16} Tr \left(\mathcal{D}_\mu U^\dagger \mathcal{D}_\mu U \right) \tag{1.1}$$

where

$$U = \exp \left(\frac{2iT^s \pi^s}{v} \right) \tag{1.2}$$

with $v = 246\ GeV$.

$$\mathcal{D}_\mu U = \partial_\mu U + \mathcal{A}_\mu U - U \mathcal{B}_\mu \tag{1.3}$$

where

$$\begin{aligned} \mathcal{A}_\mu &= W_\mu + \hat{B}'_\mu + G_\mu & \mathcal{B}_\mu &= \hat{B}_\mu + \hat{B}'_\mu + G_\mu \\ W_\mu &= igT^a W^a_\mu & \hat{B}_\mu &= ig' T^3 B_\mu \\ \hat{B}'_\mu &= ig' \frac{T_D}{\sqrt{3}} B_\mu & G_\mu &= i \frac{g_s}{\sqrt{2}} T^\alpha_8 G^\alpha_\mu \end{aligned} \tag{1.4}$$

In Eq. (1.4), W^a_μ $(a = 1, 2, 3)$, B_μ and G^α_μ $(\alpha = 1, \cdots, 8)$, are the usual $G_W = SU(3)_c \times SU(2)_L \times U(1)_y$ gauge fields.

- Decompose the matrix U according to

$$U = \begin{pmatrix} U^{ij}_{uu} & U^{ij}_{ud} & U^k_{u\nu} & U^k_{ue} \\ U^{ij}_{du} & U^{ij}_{dd} & U^k_{d\nu} & U^k_{de} \\ U^l_{\nu u} & U^l_{\nu d} & U_{\nu\nu} & U_{\nu e} \\ U^l_{eu} & U^l_{ed} & U_{e\nu} & U_{ee} \end{pmatrix} \tag{1.5}$$

The indices i, j, k and l are color indices running from 1 to 3.

- We write the most general Yukawa coupling invariant with respect to G_W involving 3rd generation fermions and (as needed for the $\mu^+\mu^-$ collider) muons.

(As usual, Yukawa couplings $\propto$ corresponding fermionic masses.)

$$
\begin{aligned}
\mathcal{L}_Y = & - m_1 \left(\bar{t}^i_R U^{\dagger ij}_{uu} t^j_L + \bar{t}^i_R U^{\dagger ij}_{du} b^j_L + h.c. \right) \\
& - m_2 \left(\bar{b}^i_R U^{\dagger ij}_{ud} t^j_L + \bar{b}^i_R U^{\dagger ij}_{dd} b^j_L + h.c. \right) \\
& - m_4 \left(\bar{\tau}_R U^{\dagger}_{\nu e} \nu_{\tau L} + \bar{\tau}_R U^{\dagger}_{ee} \tau_L + h.c. \right) \\
& - m_4^{(2)} \left(\bar{\mu}_R U^{\dagger}_{\nu e} \nu_{\mu L} + \bar{\mu}_R U^{\dagger}_{ee} \mu_L + h.c. \right) \\
& - m_5 \left(\bar{t}^i_R U^{\dagger jj}_{uu} t^i_L + \bar{t}^i_R U^{\dagger jj}_{du} b^i_L + h.c. \right) \\
& - m_6 \left(\bar{b}^i_R U^{\dagger jj}_{ud} t^i_L + \bar{b}^i_R U^{\dagger jj}_{dd} b^i_L + h.c. \right) \\
& - m_7 \left(\bar{t}^i_R U^{\dagger}_{\nu\nu} t^i_L + \bar{t}^i_R U^{\dagger}_{e\nu} b^i_L + h.c. \right) \\
& - m_9 \left(\bar{b}^i_R U^{\dagger}_{\nu e} t^i_L + \bar{b}^i_R U^{\dagger}_{ee} b^i_L + h.c. \right) \\
& - m_{10} \left(\bar{\tau}_R U^{\dagger jj}_{ud} \nu_{\tau L} + \bar{\tau}_R U^{\dagger jj}_{dd} \tau_L + h.c. \right) \\
& - m_{10}^{(2)} \left(\bar{\mu}_R U^{\dagger jj}_{ud} \nu_{\mu L} + \bar{\mu}_R U^{\dagger jj}_{dd} \mu_L + h.c. \right) \\
& - m_{11} \left[\bar{t}_R \lambda^\alpha \begin{pmatrix} U^\dagger_{uu} & U^\dagger_{du} \end{pmatrix} \begin{pmatrix} \lambda^\alpha & 0 \\ 0 & \lambda^\alpha \end{pmatrix} \begin{pmatrix} t_L \\ b_L \end{pmatrix} + h.c. \right] \\
& - m_{12} \left[\bar{b}_R \lambda^\alpha \begin{pmatrix} U^\dagger_{ud} & U^\dagger_{dd} \end{pmatrix} \begin{pmatrix} \lambda^\alpha & 0 \\ 0 & \lambda^\alpha \end{pmatrix} \begin{pmatrix} t_L \\ b_L \end{pmatrix} + h.c. \right] . \qquad (1.6)
\end{aligned}
$$

From the $\mathcal{O}(1)$ terms in the expansion of $\mathcal{L}_Y$

$$
\begin{aligned}
m_t &= m_1' + m_7 \\
m_b &= m_2' + m_9 \\
m_\tau &= m_4 + 3m_{10} \\
m_\mu &= m_4^{(2)} + 3m_{10}^{(2)} \\
m_{\nu_\tau} &= m_{\nu_\mu} = 0 \, , \qquad (1.7)
\end{aligned}
$$

where

$$
m_1' \equiv m_1 + 3m_5 + \frac{16}{3} m_{11} \, , \quad m_2' \equiv m_2 + 3m_6 + \frac{16}{3} m_{12} \, . \qquad (1.8)
$$

Note that the fermion masses provide constraints on the independent parameters appearing in $\mathcal{L}_Y$.

In the (U, D, N, E) model, the U_{uu}, U_{dd}, $U_{\nu\nu}$ and U_{ee} entries above come from techni-U, D, N and E fermion propagator loop corrections, respectively, mediated by Extended Technicolor (ETC) Gauge Bosons.

- Define:

$$P^0 = \frac{1}{\sqrt{12}}(3E\overline{E} - D\overline{D})\,, \tag{1.9}$$

$$P^{0\prime} = \frac{1}{\sqrt{12}}(U\overline{U} - 3N\overline{N})\,, \tag{1.10}$$

which are purely $T_3 = -1/2$ and $T_3 = +1/2$ weak-isospin states, respectively.

- Expanding to first order in $1/v$, we have

$$\begin{aligned} U^{ij}_{uu} &\sim \delta^{ij}\left[1 + \frac{i}{v}\sqrt{6}\frac{P^{0\prime}}{3}\right] + \ldots \\ U^{ij}_{dd} &\sim \delta^{ij}\left[1 - \frac{i}{v}\sqrt{6}\frac{P^{0}}{3}\right] + \ldots \\ U_{\nu\nu} &\sim \left[1 - \frac{i}{v}\sqrt{6}P^{0\prime}\right] + \ldots \\ U_{ee} &\sim \left[1 + \frac{i}{v}\sqrt{6}P^{0}\right] + \ldots\,. \end{aligned} \tag{1.11}$$

Non-neutral entries (U^{ij}_{ud}, $U_{\nu e}$ *etc.*) contain neither $\mathcal{O}(1)$ terms nor neutral P^0 and $P^{0\prime}$ fields (but, rather, contain charged PNGB's) in their $1/v$ expansion.

- In a multi-scale technicolor model, the above would be generalized by writing $\mathcal{L}_g$ and $\mathcal{L}_Y$ as sums of terms involving different v_i's, where each term would contain a U_i that depends on a subset of the π^s fields. Discussion to follow unaltered except v could be smaller.

- Evaluate one-loop effective potential (think of loops of normal quarks and leptons) with couplings as determined from above effective Lagrangian structure.

  $\Rightarrow$

  $$m^2_{P0}(\mathrm{one-loop}) = \frac{4\Lambda^2}{\pi^2 v^2}\rho_8\,, \quad m^2_{P0\prime}(\mathrm{one-loop}) = \frac{4\Lambda^2}{\pi^2 v^2}\rho_7\,, \quad (1.12)$$

  where

  $$\rho_8 = 2m_2' m_9 + 2m_4 m_{10} + 2m_4^{(2)} m_{10}^{(2)}\,, \quad \rho_7 = 2m_1' m_7 \qquad (1.13)$$

  and Λ is the UV cut-off, situated in the TeV region. We also note that $m^2_{P\pm} = \frac{1}{2}(m^2_{P0} + m^2_{P0\prime})$.

  m_{P0} comes only from the terms involving b, τ and μ in $\mathcal{L}_Y$.

  $m_{P0\prime}$ comes only from terms involving the t.

  Terms proportional to m_i^2 (*e.g.* $m_2'^2$, m_9^2, $\ldots$ contributions to m^2_{P0}) are absent due to a cancellation.

- In the (U, D, N, E) one-family model,

  $$m^2_{P0} = m^2_{D,E}\,, \qquad m^2_{P0\prime} = m^2_{U,N}\,. \qquad (1.14)$$

  where $m^2_{U,N}$ is the contribution coming from $\langle U\overline{U}\rangle\langle N\overline{N}\rangle$ (*e.g.* $m_1 m_7$ term) and $m^2_{D,E}$ (*e.g.* $m_2 m_9$ term) is the contribution from $\langle D\overline{D}\rangle\langle E\overline{E}\rangle$.

  - $\langle D\overline{D}\rangle$ and $\langle E\overline{E}\rangle \Rightarrow m_b$.
  - $\langle U\overline{U}\rangle$ and $\langle N\overline{N}\rangle \Rightarrow m_t$.

– $\Rightarrow m_{P^0} \ll m_{P^{0\prime}}$,

as implicit in Eqs. (1.7), (1.12) and (1.13).

- **A very crucial point:** P^0 and $P^{0\prime}$ are the mass eigenstates, and not, as implicitly assumed in most earlier studies, the isovector and isosinglet combinations:

$$\tilde{\pi}_3 = \frac{1}{\sqrt{24}}(U\overline{U} - D\overline{D} - 3N\overline{N} + 3E\overline{E})\,, \tag{1.15}$$
$$\pi_D = \frac{1}{\sqrt{24}}(U\overline{U} + D\overline{D} - 3N\overline{N} - 3E\overline{E})\,, \tag{1.16}$$

respectively.

- Additional contributions to the technilepton–techniquark operators (such as $\langle D\overline{D}\rangle\langle E\overline{E}\rangle$) can come from lepto-quark type gauge bosons. But these can be shown to preserve the P^0 and $P^{0\prime}$ as eigenstates.

  All that changes is there could be a (small perhaps) addition to the $m^2_{P^0}$ and $m^2_{P^{0\prime}}$ (but still proportional to m_b^2 and m_t^2, respectively).

- Yukawa couplings:

$$\lambda_b = -\frac{\sqrt{6}}{3v}\left(m_2' - 3m_9\right)\,, \quad \lambda_\tau = \frac{\sqrt{6}}{v}\left(m_4 - m_{10}\right)\,, \quad \lambda_\mu = \frac{\sqrt{6}}{v}\left(m_4^{(2)} - m_{10}^{(2)}\right)\,. \tag{1.17}$$

  Note:

  – λ_b, m_{P^0} [Eqs. (1.12) and (1.13)], and m_b [Eq. (1.7)] all depend only on m_2' defined in Eq. (1.8).

  – $\Rightarrow$ parameters describing $T_3 = -1/2$ sector phenomenology are 6: m_2', m_4, $m_4^{(2)}$, m_9, m_{10} and $m_{10}^{(2)}$. (4 if drop μ-related $m_i^{(2)}$.)

– Yukawa couplings and fermions masses are different combinations.

$\Rightarrow$ all 4 (6) m_i can be independently determined using known $m_b, m_\tau, (m_\mu)$ and measurements of λ_b, λ_τ, (λ_μ).

$\Rightarrow$ Given a determination of the b and τ m_i, ρ_8 in Eq. (1.13) can be computed and known m_{P^0} then $\Rightarrow$ Λ through Eq. (1.12) if the LQ contribution to $m_{P^0}^2$ is small.

– ABJ anomaly induced couplings to gauge particles:

$$g_{PV_1V_2} = \frac{\alpha N_{TC} A_{PV_1V_2}}{\pi v} \epsilon_{\lambda\mu\nu\rho} p_1^\lambda \epsilon_1^\mu p_2^\nu \epsilon_2^\rho \,, \tag{1.18}$$

where for $P = P^0$ we have:

$$A_{P^0\gamma\gamma} = -\frac{4}{\sqrt{6}}\left(\frac{4}{3}\right) \tag{1.19}$$

$$A_{P^0Z\gamma} = -\frac{4}{2\sqrt{6}}\left(\frac{1-4s_W^2}{4s_Wc_W} - \frac{t_W}{3}\right) \tag{1.20}$$

$$A_{P^0ZZ} = -\frac{4}{\sqrt{6}}\left(\frac{1-2s_W^2}{2c_W^2} - \frac{t_W^2}{3}\right) \tag{1.21}$$

$$A_{P^0gg} = \frac{1}{\sqrt{6}}\,, \tag{1.22}$$

where $s_W = \sin\theta_W$, *etc.*

Importance of mass eigenstate composition:

$$A^2_{P^0\gamma\gamma} : A^2_{\pi_D\gamma\gamma} : A^2_{\tilde{\pi}_3\gamma\gamma} = 8:1:9 \quad A^2_{P^0gg} : A^2_{\pi_Dgg} : A^2_{\tilde{\pi}_3gg} = 1:2:0\,. \tag{1.23}$$

– Special parameter choice for our studies:

$$m_1' = m_7 = \frac{m_t}{2}$$
$$m_2' = m_9 = \frac{m_b}{2}$$
$$m_{10} = -m_4 = \frac{m_\tau}{2}$$

$$m_{10}^{(2)} = -m_4^{(2)} = \frac{m_\mu}{2}\,. \tag{1.24}$$

$* \Rightarrow$

$$m^2_{P^0}(\mathrm{one-loop}) = \frac{2\Lambda^2}{\pi^2 v^2} m_b^2\,, \quad m^2_{P^{0\prime}}(\mathrm{one-loop}) = \frac{2\Lambda^2}{\pi^2 v^2} m_t^2\,, \tag{1.25}$$

$\Rightarrow$

$$m_{P^0}(\mathrm{one-loop}) \sim 8\ \mathrm{GeV} \times \Lambda(\mathrm{TeV})\,. \tag{1.26}$$

For $\Lambda < 10$ TeV (as natural for third family masses and ok with FCNC in 3rd family and ok if LQ gauge bosons don't mediate normal lepton$\rightarrow$quark transitions) $m_{P^0} < m_Z$.

(NB: our general attitude is that technicolor of DSB more generally should only be for 3rd family masses. Generate 2nd families by radiative corrections . . .)

Since $m_{P^{0\prime}}/m_{P^0} \propto m_t/m_b$, $m_{P^{0\prime}} > 250$ GeV is probable.

Since $m_{P^\pm} \sim \frac{1}{\sqrt{2}}\sqrt{m^2_{P^0} + m^2_{P^{0\prime}}} \sim \frac{1}{\sqrt{2}} m_{P^{0\prime}}$, $m_{P^\pm} \gtrsim 180$ GeV is probable.

Walking technicolor: $v \rightarrow$ some fraction of $v \Rightarrow$ enhances masses and couplings.

$*$ The fermionic couplings of the P^0 corresponding to Eq. (1.24) are

$$\lambda_b = \sqrt{\frac{2}{3}}\frac{m_b}{v}\,, \quad \lambda_\tau = -\sqrt{6}\frac{m_\tau}{v}\,, \quad \lambda_\mu = -\sqrt{6}\frac{m_\mu}{v}\,. \tag{1.27}$$

- How big is N_{TC}? Above couplings are greatly enhanced for large N_{TC}.

  Main constraint is precision electroweak: from the technifermions, one computes $S \sim 0.28 N_D (N_{TC}/3)$, where N_D is the number of technidoublets ($N_D = 4$ in (U, D, N, E) model).

90% CL limit on S is about 0.2. $\Rightarrow$ looks like a problem. But, cancellations related to PGB's and technirho and techniomega type resonances can be present. Such cancellations are probably only sufficient for $N_{TC} \lesssim 4$.

2 Branching Ratios and Width of the P^0

- Not surprisingly, the $b\overline{b}$ mode is important, but of at least equal interest is the large $B(P^0 \to gg)$ and $B(P^0 \to \gamma\gamma)$ as m_{P^0} gets large. The large associated partial widths give a total $\Gamma^{\rm tot}_{P^0}$ that is bigger than for a SM-like Higgs of the same mass.

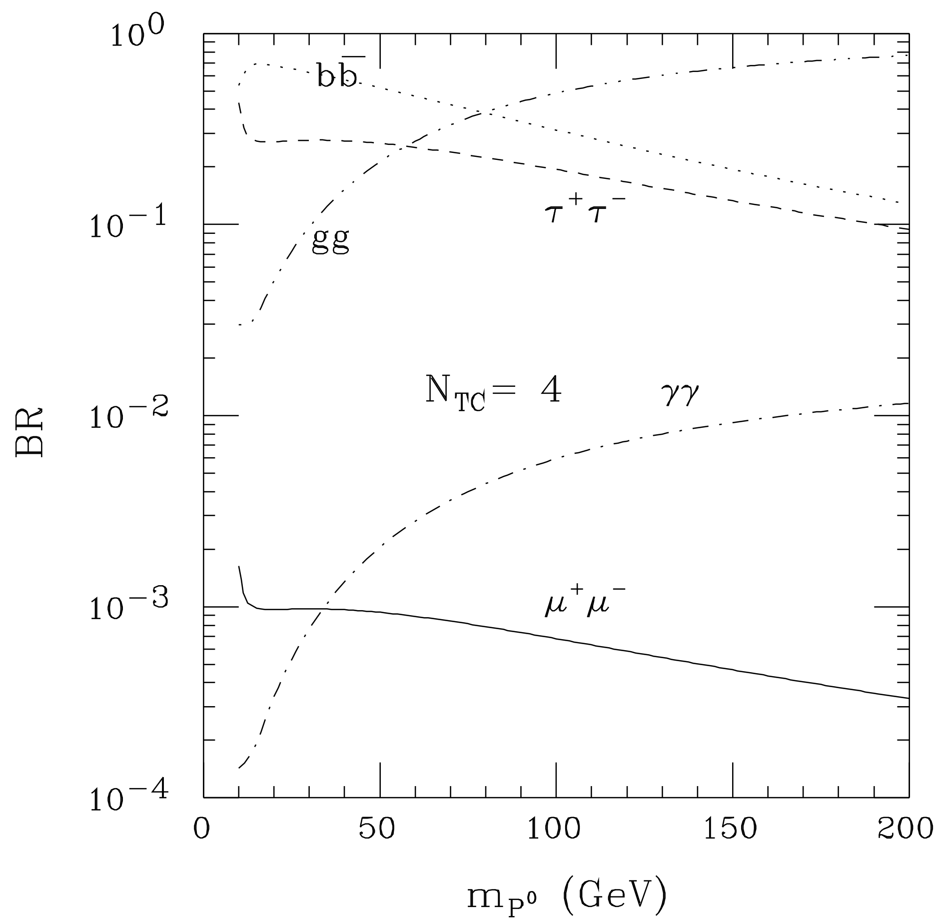

Figure 1: Branching fractions for P^0 decay into $\mu^+\mu^-$, $\tau^+\tau^-$, $b\bar{b}$, $\gamma\gamma$, and gg. We assume $N_{TC}=4$ and employ the couplings of Eqs. (1.27), (1.19) and (1.22).

- Two ratios in particular illustrate just how important the anomalous couplings are for phenomenology: $\Gamma(P^0 \to gg)B(P^0 \to \gamma\gamma)$ determines the Tevatron $\gamma\gamma$ inclusive final state rate; $\Gamma(P^0 \to \gamma\gamma)B(P^0 \to b\overline{b})$ determines the rate for the $b\overline{b}$ channel in $\gamma\gamma$ collisions.

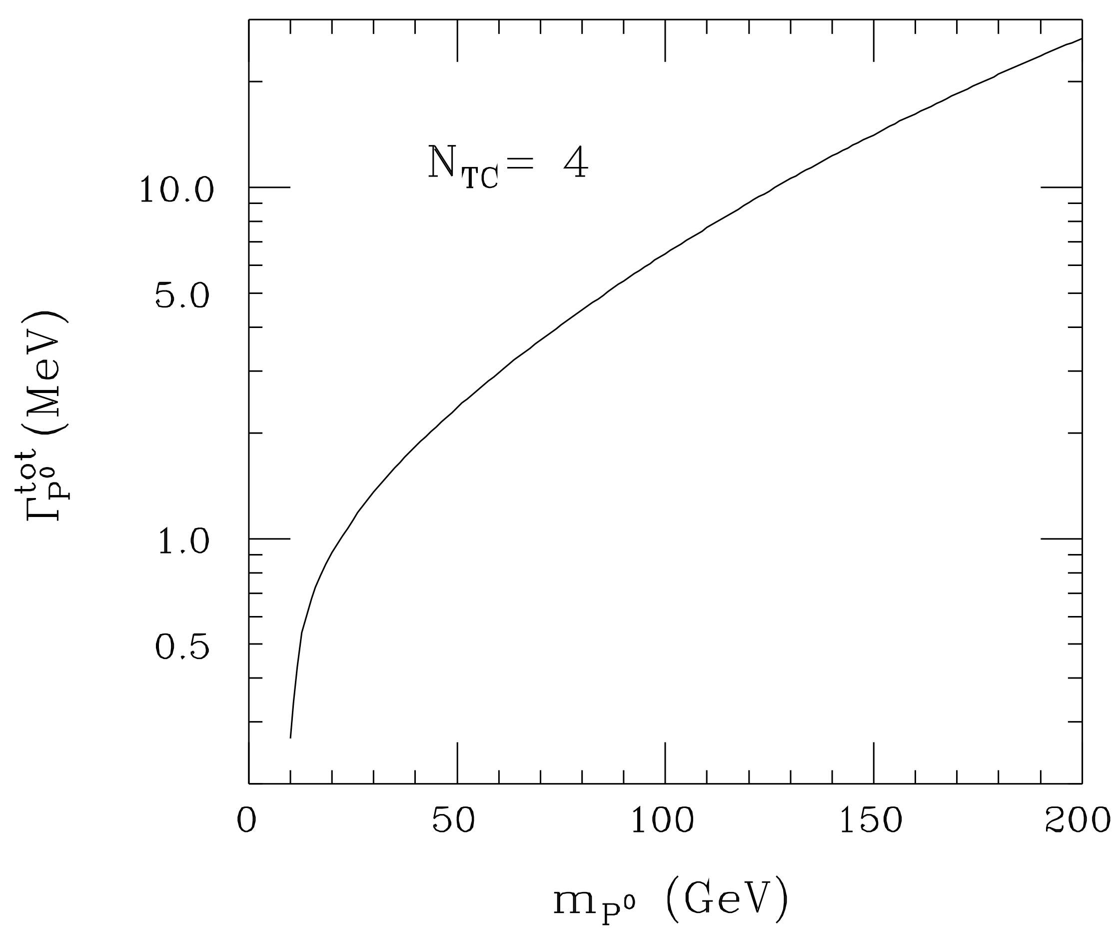

Figure 2: $\Gamma^{tot}_{P^0}$ as a function of m_{P^0}. We assume $N_{TC} = 4$ and employ the couplings of Eqs. (1.27), (1.19) (1.22).

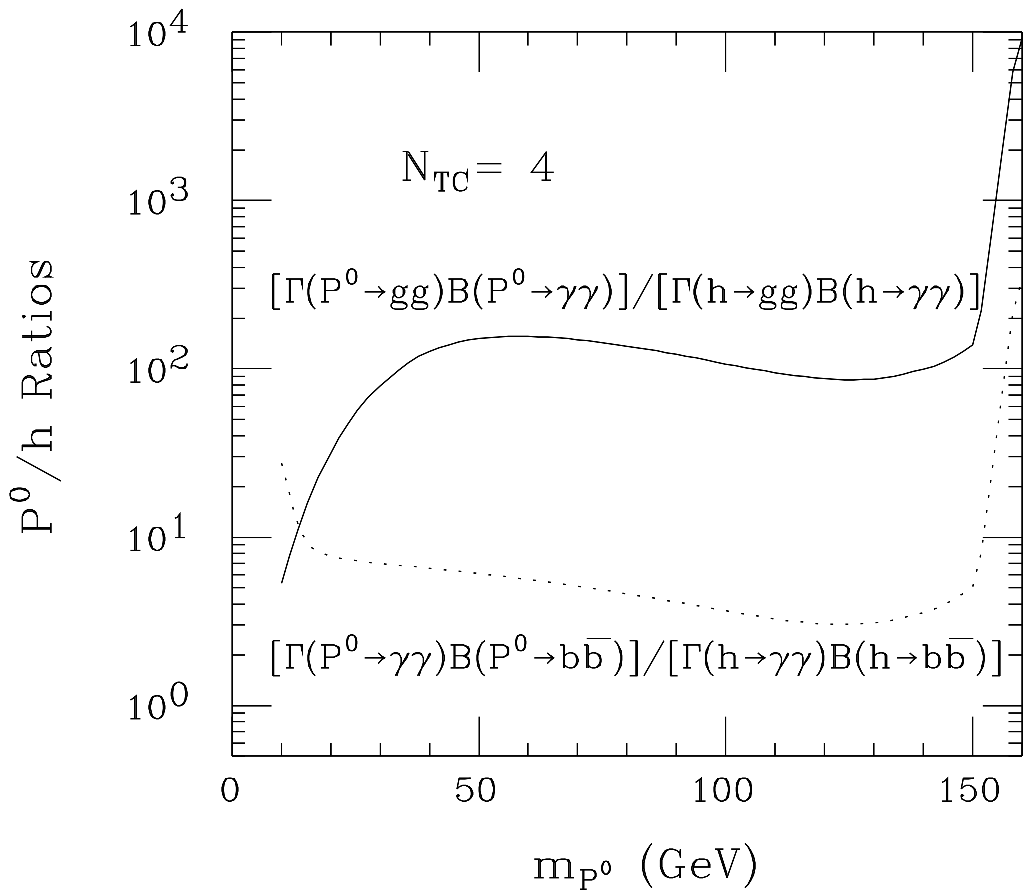

Figure 3: The ratios $[\Gamma(P^0 \to gg)B(P^0 \to \gamma\gamma)]/[\Gamma(h \to gg)B(h \to \gamma\gamma)]$ and $[\Gamma(P^0 \to \gamma\gamma)B(P^0 \to b\overline{b})]/[\Gamma(h \to \gamma\gamma)B(h \to b\overline{b})]$, where h is the SM Higgs boson, are plotted as a function of m_{P^0}, taking $m_h = m_{P^0}$. Results assume $N_{TC} = 4$ and the specific P^0 couplings of Eqs. (1.27), (1.19) and (1.22).

3 The P^0 at LEP, LEP2

- At LEP the dominant production mode is $Z \to \gamma P^0$. The width for this decay is given by

$$\Gamma(Z \to \gamma P^0) = \frac{\alpha^2 m_Z^3}{96\pi^3 v^2} N_{TC}^2 A_{P^0 Z\gamma}^2 \left(1 - \frac{m_{P^0}^2}{m_Z^2}\right), \qquad (3.1)$$

where $A_{P^0 Z\gamma}$ appeared in Eq. (1.20).

Let us we require $\Gamma(Z \to \gamma P^0) > 2 \times 10^{-6}$ GeV for the P^0 to be visible in a sample of 10^7 Z bosons. The minimum N_{TC} value required as a function of m_{P^0} is plotted in Fig. 4.

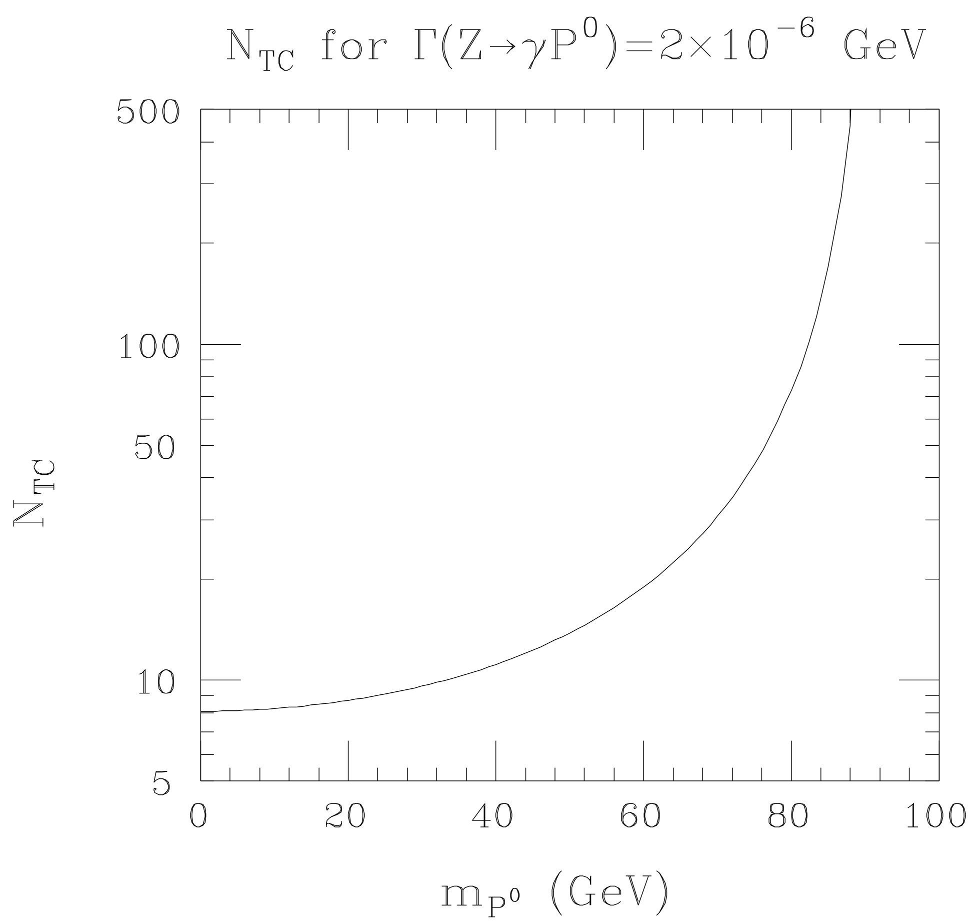

Figure 4: The value of N_{TC} required for $\Gamma(Z \to \gamma P^0) > 2 \times 10^{-6}$ GeV is plotted as a function of m_{P^0}.

$\Rightarrow N_{TC} \gtrsim 8$ is required at $m_{P^0} = 0$, rising rapidly as m_{P^0} increases.

- At LEP2, for $\sqrt{s} = 200$ GeV, requiring $20^\circ \leq \theta_\gamma \leq 160^\circ$ yields $\sigma(e^+e^- \to \gamma P^0) < 1$ fb for $N_{TC} = 4$.

  Given that $L \lesssim 0.5$ fb^{-1} is expected, $\Rightarrow$ the P^0 will not be visible at LEP2 unless N_{TC} is very large.

4 The P^0 at the Tevatron and the LHC

- At RunI, no constraints on the P^0 are possible for $N_{TC} = 4$. However, for very large $N_{TC} > 12$ the RunI data eliminates the possibility of a light P^0.

- At the Tevatron, there is a decent chance that the P^0 can be detected in RunII. At low masses, an experimental study of the γ-jet discrimination factor is needed to know if the reducible γj and jj backgrounds can be adequately suppressed.

- At the LHC, unless m_{P^0} is small, there will be no problem seeing the P^0 in the $\gamma\gamma$ inclusive mode. In fact, a highly accurate measurement (systematics limited) of $\Gamma(P^0 \to gg)B(P^0 \to \gamma\gamma)$ will be possible.

- Exactly how low in m_{P^0} the LHC can go is not certain.

  $m_{P^0} \lesssim 20$ GeV is a concern!

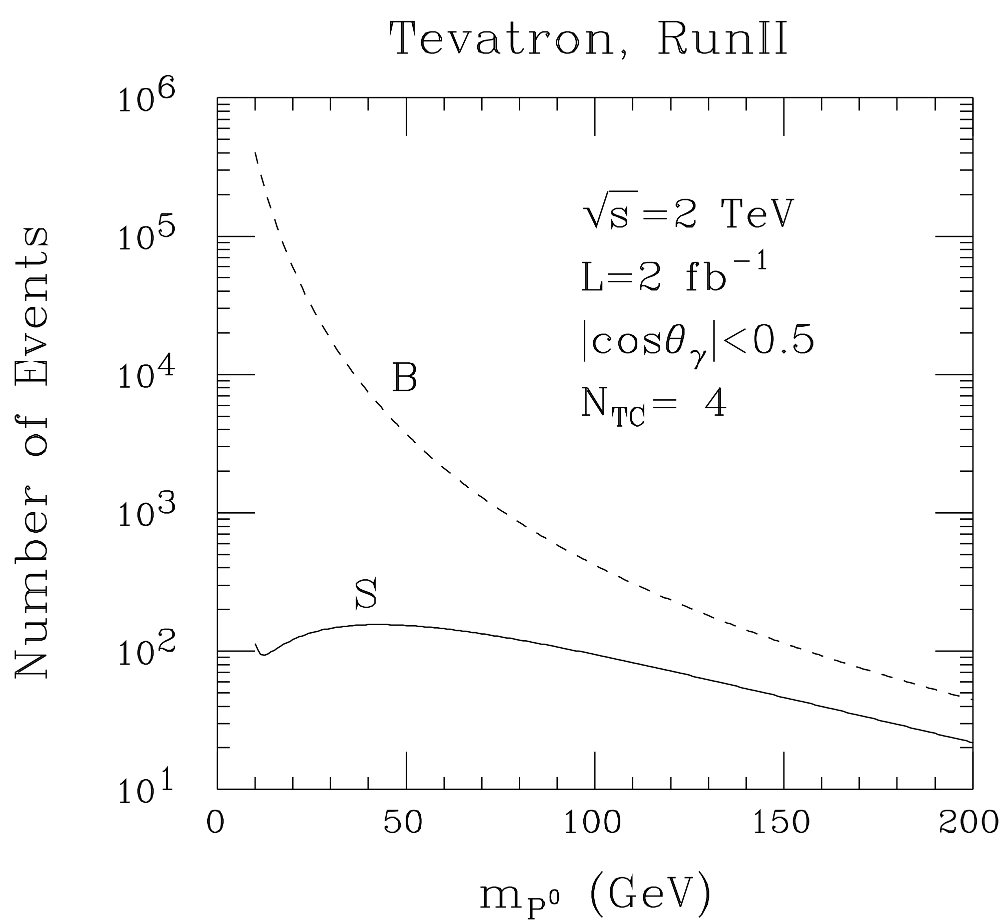

Figure 5: The $gg \to P^0 \to \gamma\gamma$ signal rate S is plotted as a function of m_{P^0} for $N_{TC} = 4$ in the case of $\sqrt{s} = 2$ TeV and $L = 2$ fb^{-1} at the Tevatron. Also shown is the irreducible background rate, B, obtained by multiplying $d\sigma(p\overline{p} \to q\overline{q} \to \gamma\gamma)/dM_{\gamma\gamma}$ by a factor of 1.5 to include the $gg \to \gamma\gamma$ loop contribution and by a mass interval size of $2\Delta M_{\gamma\gamma}$, where $\Delta M_{\gamma\gamma}$ is computed for $\Delta E_\gamma/E_\gamma = 0.135/\sqrt{E_\gamma} \oplus 0.015$. In computing both S and B, we required the final state photons to have $|\cos\theta_\gamma| < 0.5$.

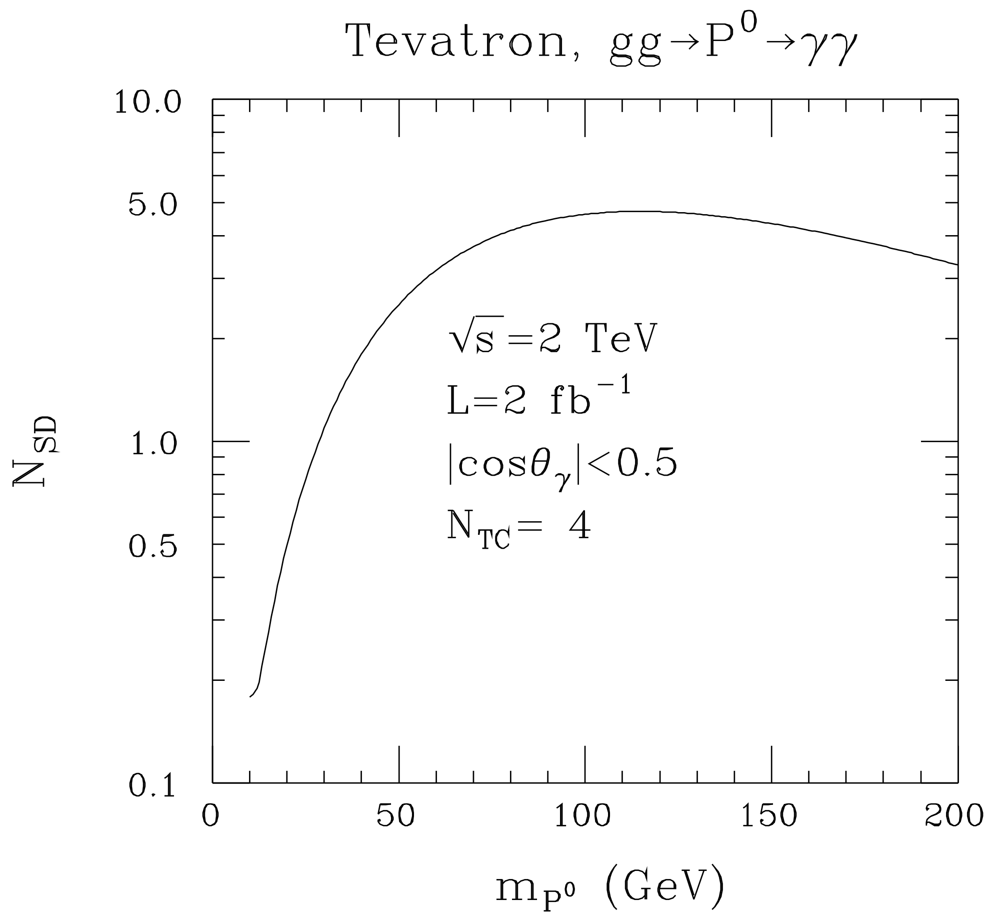

Figure 6: The $gg \to P^0 \to \gamma\gamma$ signal significance, $N_{SD} = S/\sqrt{B}$, is plotted as a function of m_{P^0} for $\sqrt{s} = 2$ TeV and $L = 2$ fb^{-1} at the Tevatron using S and B as plotted in Fig. 5.

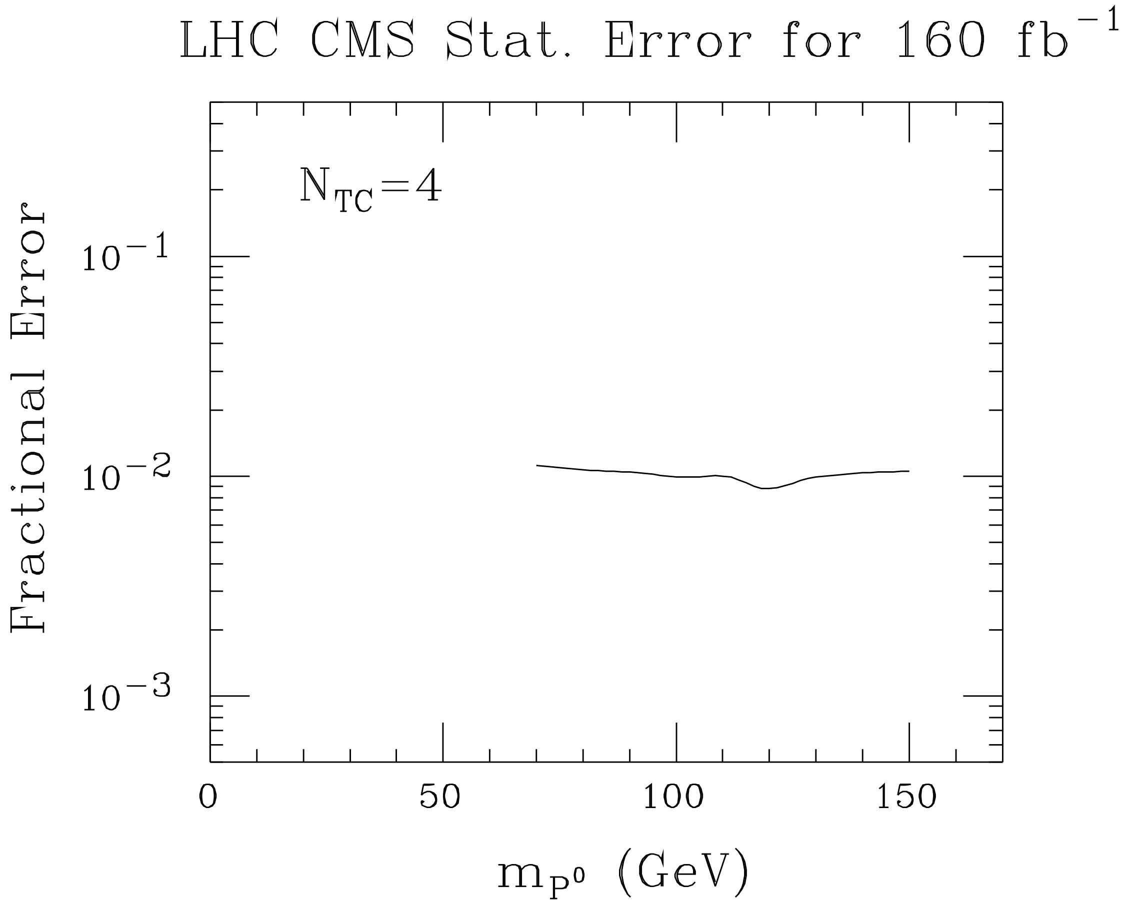

Figure 7: The fractional statistical error $(S+B)^{1/2}/S$ for the $gg \rightarrow P^0 \rightarrow \gamma\gamma$ rate, assuming $N_{TC}=4$ and $L=160$ fb^{-1} of accumulated luminosity at the LHC. Results are based on the rates quoted by CMS for the SM Higgs boson when only events containing at least two high E_T (central) or high E (forward) jets are accepted. The $gg \rightarrow P^0 \rightarrow \gamma\gamma$ signal rate S is computed from the SM Higgs rate by multiplying by the appropriate factor at each m_{P^0} as plotted in Fig. 3.

5 Results for e^+e^- collisions at the NLC

- The only potentially useful production mode is $e^+e^- \to \gamma P^0$ primarily via γ exchange. We compare the total rate to various specific channel backgrounds assuming a mass resolution of order $\Delta M = 10$ GeV in the given final state can be achieved. Various assumptions about particle-tagging efficiencies (*e.g.* b-tagging) and mis-identification probabilities have been made.

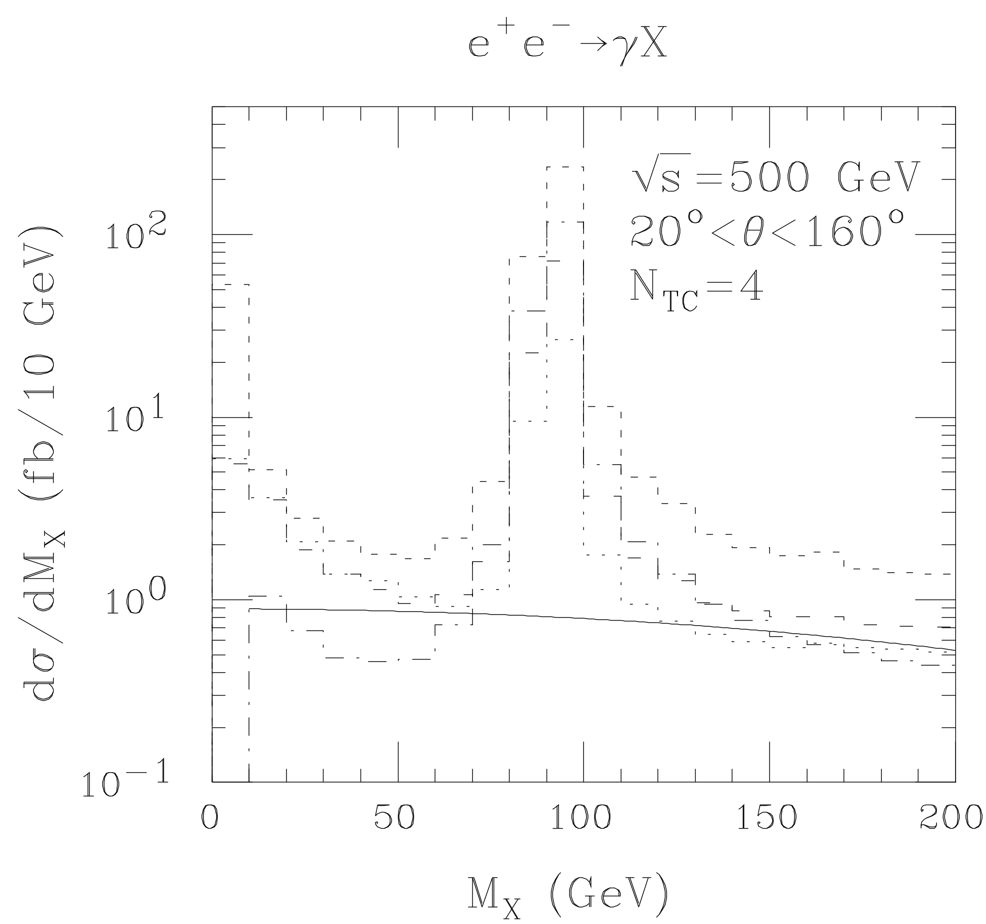

Figure 8: The cross section (in fb) for $e^+e^- \to \gamma P^0$ (solid curve) is plotted as a function of m_{P^0} in comparison to various possible backgrounds: $e^+e^- \to \gamma b\bar{b}$ (dotdash); $e^+e^- \to \gamma c\bar{c}$ (dashes); $e^+e^- \to \gamma q\bar{q}$, $q = u, d, s$ (small dashes); and $e^+e^- \to \gamma\tau^+\tau^-$ (dots). The background cross sections are integrated over a $\Delta M_X = 10$ GeV bin width (a possible approximation to the resolution that can be achieved). A cut of $20° \leq \theta \leq 160°$ has been applied to both the signal and the backgrounds. Effects due to tagging and mis-tagging are discussed in the text.

- The resulting $S/\sqrt{B}$ values for $L = 100$ fb^{-1} are not nearly as good as achievable for a SM-like Higgs boson in the Zh mode — there is no tree-level $P^0 \to ZZ$ coupling. Lowering the machine energy would probably help, and, of course, if the P^0 has already been discovered at the Tevatron or LHC, we could choose an optimum energy for running ahead of time.

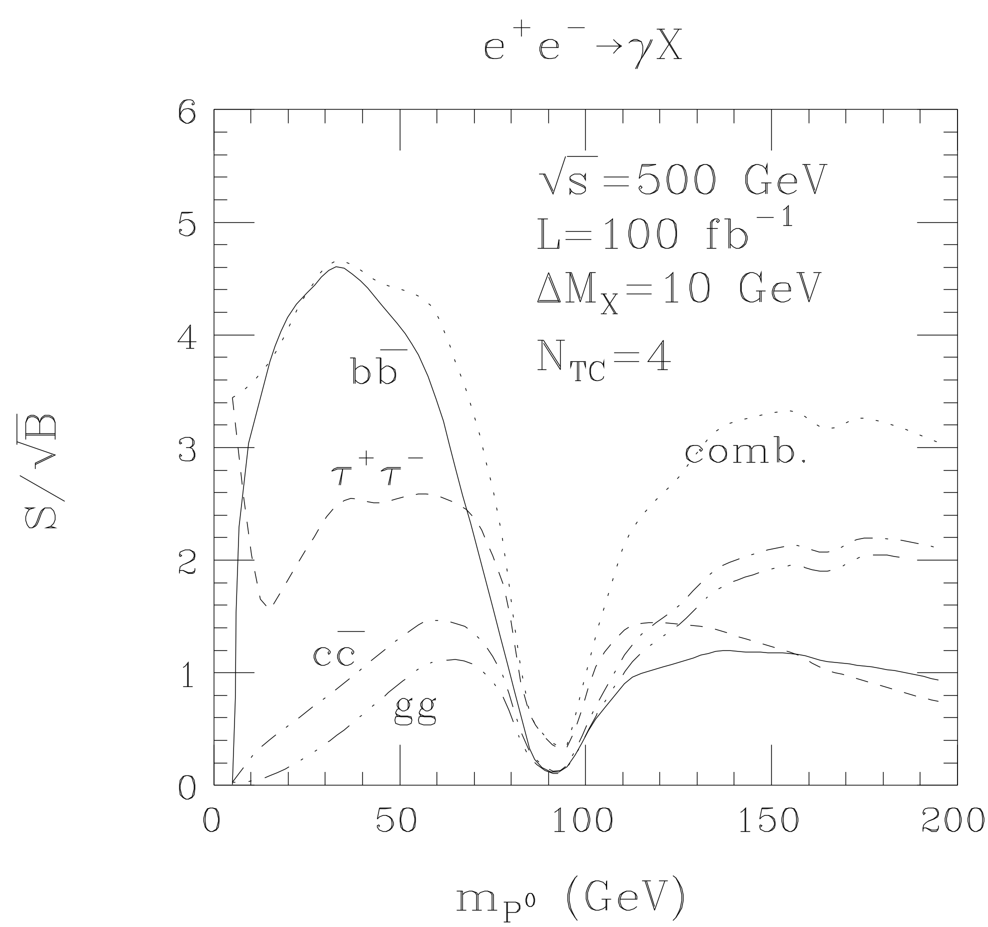

Figure 9: We consider $e^+e^- \to \gamma X$ and, for $L = 100$ fb^{-1} at $\sqrt{s} = 500$ GeV, plot the statistical significances $S/\sqrt{B}$ for a P^0 signal in various 'tagged' channels as a function of m_{P^0}. We assume mass resolution of $\Delta M_X = 10$ GeV in each channel and the channel tagging and mis-tagging probabilities discussed in the text. A cut of $20° \leq \theta \leq 160°$ has been imposed on both the signal and the backgrounds. The curve legend is: gg (dot-dot-dash); $c\overline{c}$ (dot-dash); $b\overline{b}$ (solid); $\tau^+\tau^-$ (dashes). Also shown (dots) is the largest $S/\sqrt{B}$ that can be achieved by considering all possible combinations of channels.

- Corresponding accuracies $(S+B)^{1/2}/S$ for various tagged-channel rates are relatively poor, even in the $b\overline{b}$ channel.

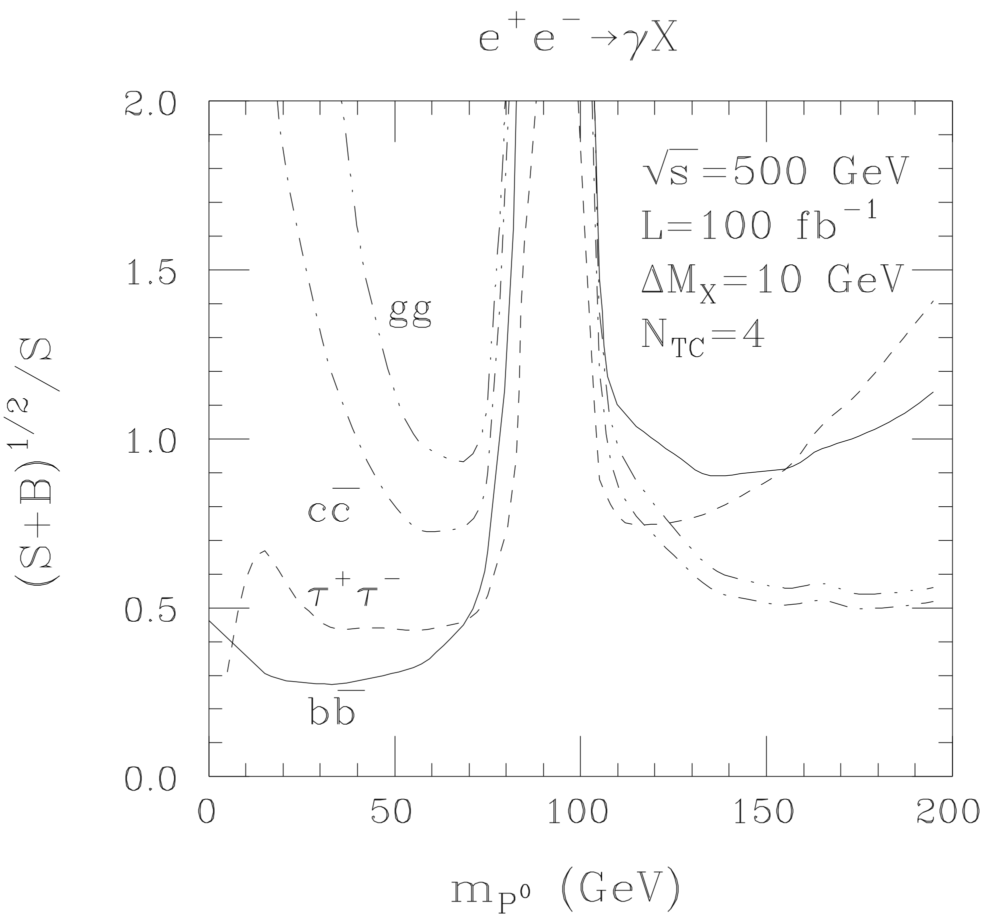

Figure 10: We consider $e^+e^- \to \gamma P^0 \to \gamma X$ production, with $L = 100\ \mathrm{fb}^{-1}$ at $\sqrt{s} = 500$ GeV, and plot the statistical error $(S+B)^{1/2}/S$ for the various 'tagged' channel rates ($X = \tau^+\tau^-$, $b\overline{b}$, $c\overline{c}$, gg) as a function of m_{P^0}. Assumptions and notation as in Fig. 9.

- Further, turning the rates into results for partial widths requires using

$$B(P^0 \to F) = \frac{\sigma(e^+e^- \to \gamma P^0) B(P^0 \to F)}{\sigma(e^+e^- \to \gamma P^0)} . \tag{5.1}$$

Must observe the P^0 inclusively in the γX final state as a peak in the recoil M_X spectrum to measure $\sigma(e^+e^- \to \gamma P^0)$.

The usual $\Delta E_\gamma / E_\gamma = 0.12/\sqrt{E_\gamma} \oplus 0.01$ yields $\pm 1\sigma$ mass windows in m_{P^0} of $[0, 78]$, $[83.5, 114]$ and $[193, 207]$ (GeV units) for $m_{P^0} = 55$, 100 and 200 GeV, respectively. If the resolution could be improved to

$\Delta E_\gamma/E_\gamma = 0.08/\sqrt{E_\gamma} \oplus 0.005$ then the mass windows for $m_{P^0} = 55$, 100 and 200 GeV become $[36, 69]$, $[91, 108]$ and $[196, 204]$, respectively. [Constant term in resolution is dominant and should be the focus for improving this particular signal.]

- Inability to get $B(P^0 \to b\bar{b})$ (or some other channel) will hurt the NLC program as described later

6 Results for $\gamma\gamma$ collisions at the NLC

- Using the well-known formula

$$N(\gamma\gamma \to R \to F) = \frac{8\pi\Gamma(R \to \gamma\gamma)B(R \to F)}{m_R^2 E_{e^+e^-}} \tan^{-1}\frac{\Gamma_{\rm exp}}{\Gamma_R^{\rm tot}}\left(1 + \langle\lambda\lambda'\rangle\right) G(y_R) L_{e^+e^-}\,, \tag{6.1}$$

  where $\langle\lambda\lambda'\rangle$ and $G(y_R \equiv m_R/E_{e^+e^-})$ depend upon the details of the $\gamma\gamma$ collision set-up. For initial discovery, choose a broad spectrum set up yielding $\langle\lambda\lambda'\rangle \sim 0.8^*$ and $G \gtrsim 1.^\dagger$

- Even for the broad spectrum case, the very large $\Gamma(P^0 \to \gamma\gamma)B(P^0 \to b\overline{b})$ compared to a SM-like Higgs means that we will get excellent results.

  Rates are large: Assume that $L_{\rm eff} \equiv G(y_{P^0})L_{e^+e^-} = 20~\mathrm{fb}^{-1}$, independent of m_{P^0}. ($G \gtrsim 1$ at the lowest masses requires lowering $\sqrt{s}$ so that $m_{P^0}/\sqrt{s} > 0.1 - 0.2$.)

  $\Rightarrow$ For the $b\overline{b}$ channel, the signal and background rates plotted give $S/\sqrt{B}$ rising from $\sim$ 8 at $m_{P^0} \sim$ 20 GeV to $\sim$ 200 at $m_{P^0} \sim$ 200 GeV.

- If m_{P^0} is already known can use use a peaked spectrum set up with $G \sim 7 - 10$ for $m_{P^0} \sim 0.8\sqrt{s}$. Measurement accuracies are very good for $b\overline{b}$.

  Rescaling the results of a recent Higgs study (which assumes a peaked luminosity distribution with a total of $L = 10~\mathrm{fb}^{-1}$) for the 106 GeV $\leq$

---

*To suppress the $q\overline{q}$ backgrounds; must introduce cuts to eliminate extra g radiation.

†Choose laser polarizations P and P' and e^+e^- beam helicities λ_e and λ_e' in the configuration $2\lambda_e P \sim +1$, $2\lambda_e' P' \sim +1$, $PP' \sim +1$.

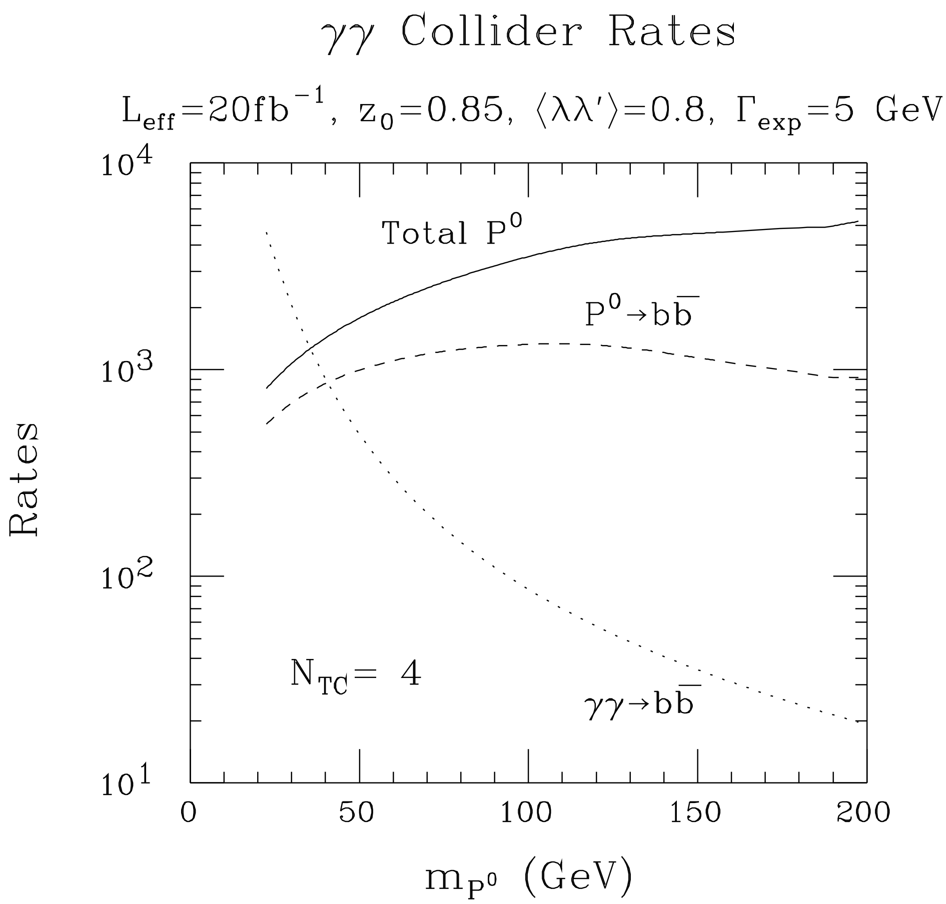

Figure 11: We consider $\gamma\gamma$ collisions for $L_{\rm eff} = 20\ {\rm fb}^{-1}$ (assumed independent of m_{P^0}), with an angular cut of $|\cos\theta| < 0.85$ applied to the two-particle final state. An experimental resolution $\Gamma_{\rm exp} = 5$ GeV is assumed in the final state. We plot, as a function of m_{P^0}: the total $\gamma\gamma \to P^0$ production rate (solid); the rate for $\gamma\gamma \to P^0 \to b\bar{b}$ (dashes); and the $\gamma\gamma \to b\bar{b}$ irreducible background rate (dots). $N_{TC} = 4$ is assumed.

$m_{jj} \leq 126$ GeV mass window to the case of the $P^0 \Rightarrow S \sim 5640$ compared to $B \sim 325$, after angular, topological tagging and jet cuts. $\Rightarrow (S+B)^{1/2}/S = 1.5\%$. Systematic errors will probably dominate.

- Other channels? $\gamma\gamma \to P^0 \to \tau^+\tau^-$ and gg will also have large event rates.
  - Backgrounds are probably too large in the gg final state.
  - Backgrounds in the $\tau^+\tau^-$ channel are not large, but there is no sharp mass peak in this channel. Still, if one configures the ma-

chine energy and $\gamma\gamma$ collision set-up so that the $\gamma\gamma$ luminosity is very peaked at an already known value of m_{P^0}, a reasonably precise measurement of $\Gamma(P^0 \to \gamma\gamma)B(P^0 \to \tau^+\tau^-)$ might prove possible.

– For the broad spectrum assumptions, the $\gamma\gamma \to P^0 \to \gamma\gamma$ event rate ranges from a low of ~ 20 at $m_{P^0} \sim 100$ GeV to ~ 50 at $m_{P^0} \sim 200$ GeV.

  Bigger rates for optimized set up.

  Presumably the (one-loop) irreducible $\gamma\gamma \to \gamma\gamma$ background is quite small.

  Jets that fake photons will be dominant background.

  A detailed study is needed.

  Potential importance $\Rightarrow$ determine total P^0 width, $\Gamma^{\rm tot}_{P^0}$.

  * Rate for $\gamma\gamma \to P^0 \to \gamma\gamma \propto \Gamma(P^0 \to \gamma\gamma)B(P^0 \to \gamma\gamma) = [\Gamma(P^0 \to \gamma\gamma)]^2/\Gamma^{\rm tot}_{P^0}$.
  * Rate for $\gamma\gamma \to P^0 \to b\bar{b} \propto \Gamma(P^0 \to \gamma\gamma)B(P^0 \to b\bar{b})$.
  * If $B(P^0 \to b\bar{b})$ known from e^+e^- collisions (very difficult as we saw) then extract $\Gamma(P^0 \to \gamma\gamma)$ from $b\bar{b}$ rate and use it to extract $\Gamma^{\rm tot}_{P^0}$ from $\gamma\gamma$ final state rate.

7 P^0 production at a muon collider

- Note: only P^0 has $\mu^+\mu^-$ coupling; not the $P^{0\prime}$.
- Good measurements of rates in the $b\overline{b}$, $\tau^+\tau^-$, $c\overline{c}$ and gg s-channel production final states will be possible.
- An accurate measurement of the total width $\Gamma^{\rm tot}_{P^0}$ will also be possible.
- The challenge for the NLC will be to show that an equally good job on channel rates can be done using the $\gamma\gamma$ collider mode of operation.
- Is there any hope to get comparable NLC accuracy for $\Gamma^{\rm tot}_{P^0}$?

8 Using the NLC measurements to determine the effective low-energy theory

The experimentally well-measured quantities that could be available to us without the muon collider are:

- $\Gamma(P^0 \to gg)B(P^0 \to \gamma\gamma)$ from the LHC;
- $\Gamma(P^0 \to \gamma\gamma)B(P^0 \to b\overline{b}, \tau^+\tau^-, \gamma\gamma)$ from the $\gamma\gamma$ collider.

First, suppose we had a determination of $\Gamma_{P^0}^{\rm tot}$. The measured quantities listed have parameter dependences:

$$\Gamma(P^0 \to gg)\Gamma(P^0 \to \gamma\gamma) \propto \frac{N_{TC}^4}{v^4}\,; \tag{8.1}$$

$$\Gamma(P^0 \to \gamma\gamma)\Gamma(P^0 \to b\overline{b}) \propto \frac{N_{TC}^2}{v^2}\frac{\left[4m_2' - 3m_b\right]^2}{v^2}\,; \tag{8.2}$$

$$\Gamma(P^0 \to \gamma\gamma)\Gamma(P^0 \to \tau^+\tau^-) \propto \frac{N_{TC}^2}{v^2}\frac{\left[\frac{4}{3}m_4 - \frac{1}{3}m_\tau\right]^2}{v^2}\,; \tag{8.3}$$

$$\Gamma(P^0 \to \gamma\gamma)\Gamma(P^0 \to \gamma\gamma) \propto \frac{N_{TC}^4}{v^4}\,. \tag{8.4}$$

However, in reality, each of the above must be divided by $\Gamma_{P^0}^{\rm tot}$ to get actual measured rates. However, to the extent that the gg, $\tau^+\tau^-$ and $b\overline{b}$ final states dominate the P^0 decays, $\Gamma_{P^0}^{\rm tot}$ is a function of the same three quantities:

- N_{TC}/v;
- $|4m_2' - 3m_b|/v$;
- $|\frac{4}{3}m_4 - \frac{1}{3}m_\tau|/v$;

Strategy?

- First check consistency of $gg \to \gamma\gamma$ rate relative to $\gamma\gamma \to \gamma\gamma$ rate to verify anomalous coupling ratios. (comforting, but not crucial.)

- If successful, use remaining 3 independent measurements to extract above quantities.

- In the context of the present model, $v = 246$ GeV and the above determination of N_{TC}/v would then yield a result for N_{TC}.

- For any value of v, two-fold ambiguities in m_2' and m_4 will remain. For each choice:

  – Determine m_9 and m_{10} using $m_b = m_2' + m_9$ and $m_\tau = m_4 + 3m_{10}$;

  – Compute $\rho_8 = 2m_2'm_9 + 2m_4m_{10}$;

  – Compute a 'one-loop value' for Λ using ρ_8 and $m_{P^0}^2 = \frac{4\Lambda^2}{\pi^2 v^2}\rho_8$.

- To eliminate ambiguities, could test against one-loop dominance assumption:

  For our sample parameter choices of

$$(m_2' = \frac{1}{2}m_b, m_9 = \frac{1}{2}m_b)\,; \quad \text{and} \quad (m_4 = -\frac{1}{2}m_\tau, m_{10} = \frac{1}{2}m_\tau)\,. \tag{8.5}$$

  $\rho_8 = \frac{1}{2}(m_b^2 - m_\tau^2)$. The alternative m_i choices giving the same values of $|\frac{4}{3}m_4 - \frac{1}{3}m_\tau|/v$ and $|4m_2' - 3m_b|/v$, while maintaining consistency with m_b and m_τ, are:

$$(m_2' = m_b, m_9 = 0)\,; \quad \text{and/or} \quad (m_4 = m_\tau, m_{10} = 0)\,. \tag{8.6}$$

  The alternative values that emerge for ρ_8 are:

  – (1) 0 for $m_9 = m_{10} = 0$;

– (2) $\frac{1}{2}m_b^2$ for $m_9 = m_b/2$ and $m_{10} = 0$; and

– (3) $-\frac{1}{2}m_\tau^2$ for $m_9 = 0$ and $m_{10} = m_\tau/2$.

Of these, (1) and (3) are clearly unphysical. $\Rightarrow$

Neglecting LQ mass contributions, the only physically consistent value of $(m_2', m_9)/v$ would be $(\frac{1}{2}m_b, \frac{1}{2}m_b)/v$, and the only ambiguity would be between the choices $(m_4, m_{10})/v = (-\frac{1}{2}m_\tau, \frac{1}{2}m_\tau)/v$, vs. $(m_4, m_{10})/v = (m_\tau, 0)/v$.

9 Conclusions and Discussion

Theory:

- Getting the eigenstate right is crucial.
- The P^0 eigenstate is very special.

  Since its mass is $\propto m_b$, it should be much lighter than all other PNGB's; all others bring in m_t into mass formula.
- Only a few partial widths of P^0 are important and they are expressed in terms of a relatively small number of parameters of the effective Lagrangian.

Experiment:

- No limits on P^0 from LEP or LEP2 or Tevatron
- RunII has quite a decent chance for finding the P^0.
- Will almost certainly discover the P^0 at the LHC. Only problem area might be very low m_{P^0}.
- Poor accuracy anticipated for normal $e^+e^- \to \gamma P^0$ measurements means that $\gamma\gamma$ collider mode of operation will be very crucial. Only clear alternative is muon collider.

  In either case, LHC discovery tells us the mass to aim for.
- In $\gamma\gamma$ operation mode, must measure as many final states as possible, but both $b\overline{b}$ and $\tau^+\tau^-$ are certainly required; $\gamma\gamma$ and (backgrounds?) gg would be very helpful.

- If the $\gamma\gamma \to \gamma\gamma$ measurement can be made with good accuracy, then $\gamma\gamma$ collisions can allow a stand-alone analysis of the low-energy parameters related to the P^0.
- The LHC $gg \to \gamma\gamma$ measurement can provide a substitute/cross check.
- With the above measurements, many interesting parameters of the theory can be determined.
  - Unambiguous determination of N_{TC}/v.
  - Effective Yukawa Lagrangian parameters (in units of v) in down-quark/lepton sector, subject to possible ambiguities.